

Design of sharp transmission filters using band-edge resonances in one-dimensional photonic crystal hetero-structures

G. Alagappan · P. Wu

Received: 27 March 2009 / Revised version: 3 June 2009 / Published online: 18 July 2009
© Springer-Verlag 2009

Abstract This paper presents a design of sharp transmission filters using band edge resonance effects in a hetero-structure composed of one-dimensional photonic crystals with different periods. Assuming that the photonic crystals are made of identical pairs of transparent materials, the band-edge resonance occurs when the periods are distributed in a geometrical progression with a common ratio, $r = r_c$, where r_c is a known function of refractive-index modulation, incident angle and the polarization of light. The band-edge resonance results in sharp resonant peaks in the transmission spectrum, with the full width at half maximum of the peaks increasing with an increase in the number of unit cells in each photonic crystal. Furthermore, if M photonic crystals are used to construct the hetero-structure, $M - 1$ resonant peaks with the spacing between k th ($1 < k < M$) and $(k - 1)$ th peaks equal to the band gap of the k th photonic crystal form in the transmission spectrum.

PACS 42.70.Qs · 42.70.Df

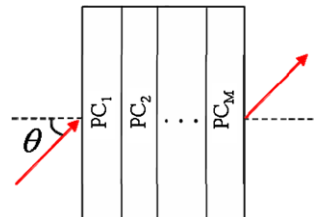
A one-dimensional (1D) photonic crystal (PC) provides a band gap—a spectral range of light reflection—for blocking light propagation in a single direction [1, 2] or omnidirections [3–5]. By appropriately introducing defects in the 1D structure, narrow line width transmission filters can be constructed. A single defect layer with a positive refractive index in the middle of a 1D PC can act as a narrow line

width filter for a fixed angle of incidence [1, 2, 6]. If the defect layer has a negative refractive index, then the filter will have additional angular filtering properties [7, 8]. Other mechanisms to implement narrow line width filters include a hybrid structure consisting of a micro-ring and a 1D PC [9] and the usage of surface modes of a 1D PC [10]. In this paper we present a new class of narrow line width filters based on band edge resonance effects in a hetero-structure of 1D PCs. The 1D PCs are assumed to be made of passive materials with positive refractive indices. The filter can be designed to have multiple wavelength channels and to operate at any angle of incidence and polarization state of the light.

Figure 1 shows a hetero-structure formed by a series of M 1D PCs with the period for the k th PC (i.e. PC_k) being p_k ($p_{k-1} < p_k < p_{k+1}$). Let us assume that each of these PCs is composed of N identical pairs of dielectric layers with refractive indices, n_1 and n_2 , with quarter-wavelength thicknesses, $p_k n_2 / (n_1 + n_2)$ and $p_k n_1 / (n_1 + n_2)$, respectively.

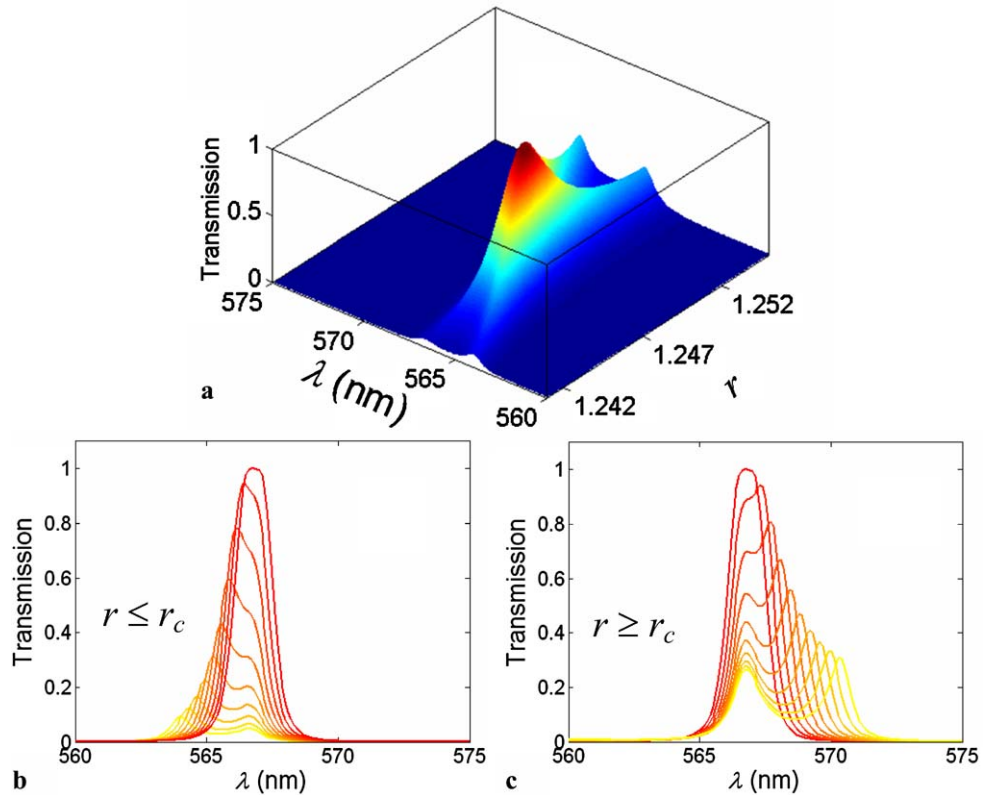
Firstly, we will examine band-edge resonance for $M = 2$ and, thereafter, a general M will be considered. With $M = 2$ we have two PCs, PC_1 and PC_2 . The periods of PC_1 and PC_2 are p_1 and p_2 ($p_2 > p_1$), respectively with the ratio p_2/p_1 being r . The lower and upper band-gap edges of the k th PC

Fig. 1 Schematic of a hetero-structure with M 1D PCs



G. Alagappan (✉) · P. Wu
Institute of High Performance Computing, 1 Fusionopolis Way,
#16-16 Connexis, Singapore 138632, Singapore
e-mail: gandhi@ihpc.a-star.edu.sg

Fig. 2 (a) Transmission as a function of r and λ for $n_1 = 1.45$, $n_2 = 2.00$, $p_1 = 150$ nm, $N = 24$ and $\theta = 0$. (b) Cross section of (a) for $r < r_c = 1.247$ ($r = 1.241$ (yellow) to $r = r_c$ (red) in step of 7.0×10^{-4}). (c) Cross section of (a) for $r > r_c$ ($r = r_c$ (red) to $r = 1.255$ (yellow) in step of 8.5×10^{-4})



are $\lambda_{-,k}$ and $\lambda_{+,k}$ ($k = 1$ or 2), respectively. These band-gap edges can be written as

$$\frac{1}{\lambda_{\pm,k}} = \frac{\omega_c}{p_k} \left(1 \mp \frac{g_n}{2} \right), \quad (1)$$

where ω_c is the normalized frequency of the band-gap center and g_n is the ratio of the widths of the normalized band-gap frequencies, $\Delta\omega$, to ω_c . Both g_n and ω_c are independent of p_k and are functions of polarization (P) and incident angle (θ) of light. The values of g_n and ω_c can be calculated using the plane wave expansion method [11] for an infinite N or employing the transfer matrix method [12] for a finite N .

When $r = 1$, the transmission spectrum of the hetero-structure will exhibit a band gap identical to band gaps of individual PCs as the upper and lower band edges of each PC coincide exactly (i.e. $\lambda_{\pm,1} = \lambda_{\pm,2}$). When r increases, $\lambda_{-,2} > \lambda_{-,1}$ and $\lambda_{+,2} > \lambda_{+,1}$ (1) and the hetero-structure will exhibit a band gap that is larger than the band gaps of individual PCs as long as $\lambda_{-,2} < \lambda_{+,1}$. Band-edge resonance occurs if the upper band edge of PC₁ coincides with the lower band edge of PC₂ (i.e. $\lambda_{-,2} = \lambda_{+,1}$). Using (1), it can be shown that when $\lambda_{-,2} = \lambda_{+,1}$, $r = r_c$, where

$$r_c = \frac{1 + g_n/2}{1 - g_n/2}. \quad (2)$$

The transmission (i.e., absolute value of transmission coefficient [1]) as a function of λ and r is calculated using the transfer matrix method [12] for a hetero-structure with $n_1 = 1.45$, $n_2 = 2.0$, $\theta = 0$, $M = 2$ and $N = 24$. The result of the calculation is shown in Fig. 2a. The peak of the transmission occurs when $r = r_c = 1.2473$. The cross sections of Fig. 2a are shown in Figs. 2b and c for r values lesser and greater than r_c , respectively. When $r < r_c$ (Figs. 2a and b), there are two peaks in the transmission spectra (these peaks disappear for $r \ll r_c$). The two transmission peaks get closer as $r \rightarrow r_c$ and reach resonance when $r = r_c$. For $r > r_c$, the two peaks separate apart with reduced transmissions (Figs. 2a and c). The resonant peaks as a function of λ for various N are displayed in Fig. 3a. As we can see from Fig. 3a, the resonant wavelength and the full width at half maximum (FWHM) of the resonant peak decrease as N increases. The plot of the FWHM as a function of N is shown in Fig. 3b and it shows that the FWHM of the resonant peak reduces exponentially as N increases.

Now let us analyze the resonance condition in (1) in more detail. Figure 4a shows the off-normal band structure [2–4] for $n_1 = 1.45$ and $n_2 = 2.0$, calculated using the plane wave expansion method [11], assuming that N is infinite. The off-normal wave vector, k_y , is related to θ by $\omega \sin \theta = k_y$, where ω is the normalized frequency. As we can see from Fig. 3a, when θ increases, the band gap of s (electric field perpendicular to the plane of incidence) polarization in-

Fig. 3 (a) Band-edge resonant peaks as a function of λ and N for $n_1 = 1.45$, $n_2 = 2.00$, $p_1 = 150$ nm and $\theta = 0$. (b) FWHM and logarithm of FWHM (i.e. $\ln(\text{FWHM})$) as a function of N for peaks in (a)

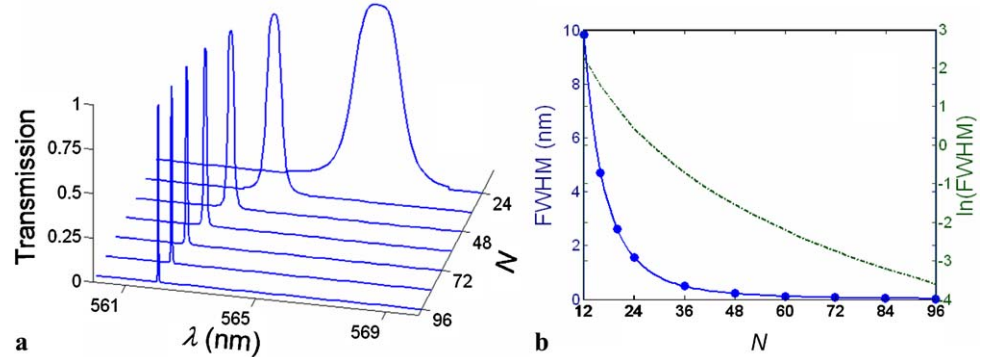
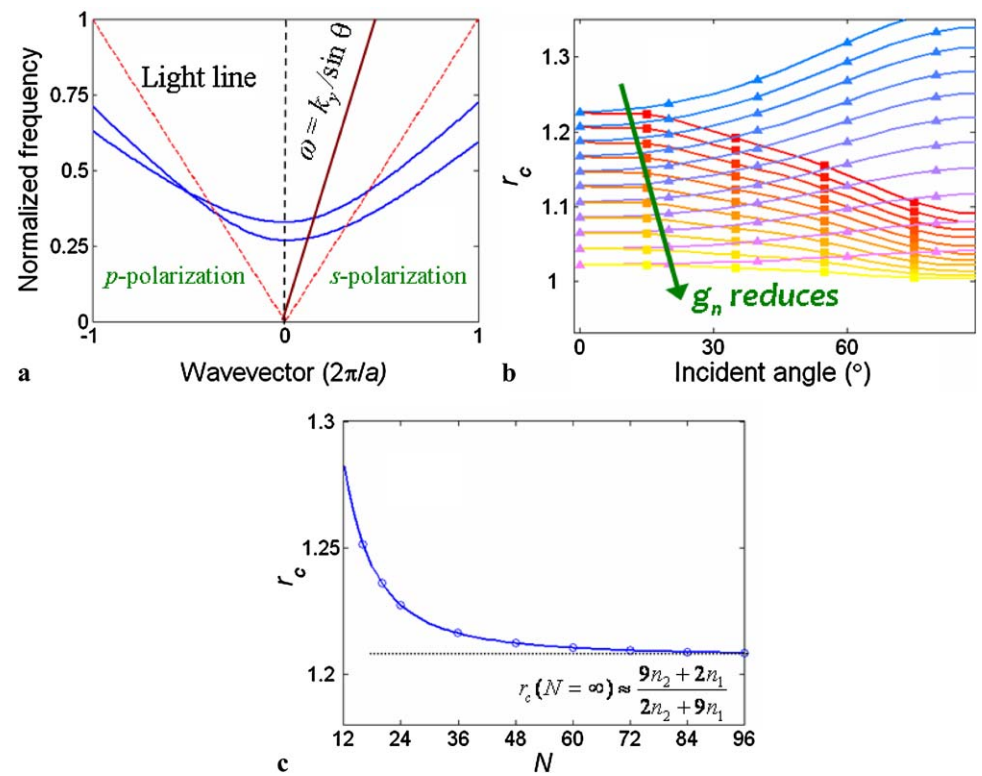


Fig. 4 (a) Photonic band structure with off-normal wave vectors, k_y , for $n_1 = 1.45$ and $n_2 = 2.00$. The lower and upper band edges of the first band gap are plotted with the blue lines for p (left-hand axis) and s (right-hand axis) polarizations. (b) r_c ($N = \infty$) versus θ for s and p polarizations with $n_1 = 1.45$ and n_2 being reduced from 2.00 to 1.50. Key for s polarization: $n_2 = 2.00$ (blue) is decreased to 1.50 (pink) in step of 0.05. Key for p polarization: $n_2 = 2.00$ (red) is decreased to 1.50 (yellow) in step of 0.05. (c) r_c as a function of N for $n_1 = 1.45$, $n_2 = 2.00$ and $\theta = 0$



creases, while for p (electric field is parallel to the plane of incidence) polarization it reduces. Therefore, g_n rises for s polarization and drops for p polarization as θ increases. The derivative of (2) with respect to g_n is always positive and, hence, when θ increases, r_c will rise for s polarization and will drop for p polarization. Variations in r_c as a function of θ are shown in Fig. 4b for s and p polarizations for various g_n . When $\theta = 0$, the band structures of both polarizations are degenerate and, assuming a small refractive-index modulation with $n_2 > n_1$, $g_n \approx [2(n_2 - n_1)/\pi(n_2 + n_1)]$ [1, 5]. Consequently, when $\theta = 0$, r_c can be simplified as

$$r_c(\theta = 0) \approx \frac{9n_2 + 2n_1}{2n_2 + 9n_1}. \quad (3)$$

In deriving the expression in (3), the approximation, $(\pi - 2)/(\pi + 2) \approx 2/9$ has been used. For a very small refractive-

index modulation, $g_n \rightarrow 0$ (or $n_2 \approx n_1$), and hence $r_c \rightarrow 1$ (see (1) and (3) and Fig. 4b). In Fig. 4a, the point at which the band gap of p polarization becomes zero lies below the light line. If this point lies above the light line (e.g. if $n_1 = 1.45$ and $n_2 = 1.00$), then g_n of p polarization becomes zero when θ equals the Brewster angle, θ_B [3, 4], and r_c of p polarization becomes 1 (1) at this angle. Further, in this case, the band-edge resonance will not occur for $\theta < \theta_B$.

For a finite N , in general g_n is larger than g_n of the infinite N [1] and therefore r_c (finite N) $>$ r_c (infinite N) (1). The dependence of r_c on N is shown in Fig. 4c for $\theta = 0$, $n_1 = 1.45$ and $n_2 = 2.00$. As can be seen from the figure, r_c reduces as N increases. For large values of N , r_c can be approximated using (3).

The band-edge resonance seen for a hetero-structure of two PCs can be generalized to a hetero-structure composed

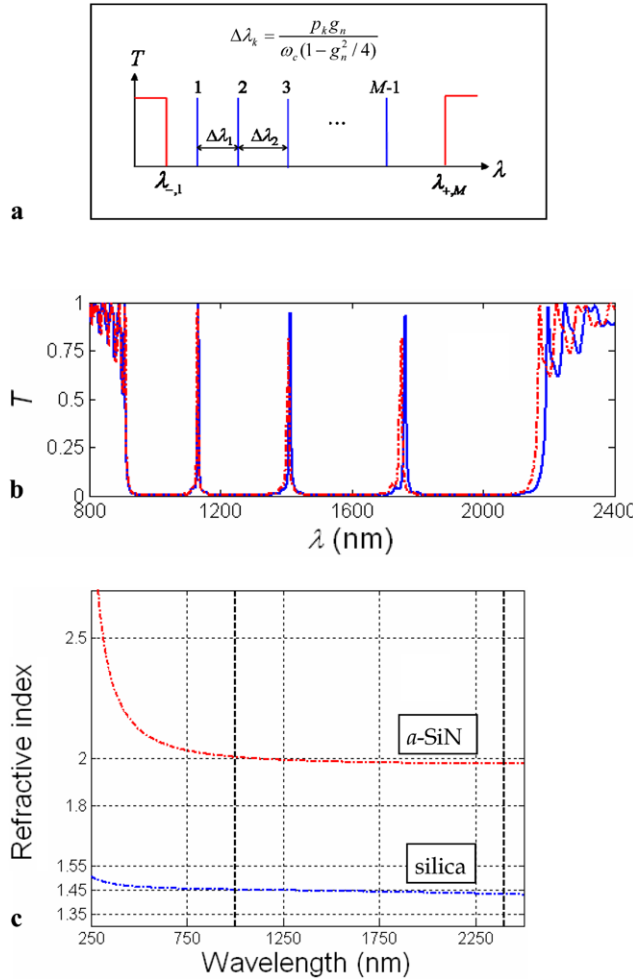


Fig. 5 (a) The general features of the transmission spectrum for a hetero-structure of M 1D PCs with the periods being distributed in a geometrical progression of a common ratio, $r = r_c$. (b) Transmission spectra for a hetero-structure with $M = 4$, $\theta = 0$, $n_1 = 1.45$, $n_2 = 2.00$, $p_1 = 300$ nm, $N = 24$ and $r = r_c = 1.247$. Blue—dispersions in (c) excluded. Red—dispersions in (c) included. (c) Refractive-index dispersions of silica [13] and amorphous silicon nitride [14]. The black lines point to the wavelengths 1000 and 2400 nm

of M 1D PCs. A schematic illustration of the resonant peaks in the hetero-structure containing multiple 1D PCs is shown in Fig. 5a. Assuming that the period of the k th PC, PC_k ($1 < k < M$), is p_k ($p_{k+1} > p_k$), the resonance requires that $\lambda_{+,k} = \lambda_{-,k+1}$. Therefore, in order have resonance at all adjacent band edges, $p_{k+1}/p_k = r_c$ (2), which is a constant. As r_c is a constant independent of p_k , the resonance in fact occurs in a series of 1D PCs with the periods being distributed in a geometrical progression of a common ratio r_c (2). The transmission spectrum of such a hetero-structure will have $M - 1$ resonant peaks with the spacing between the k th and $(k - 1)$ th peaks equal to the band gap of the k th PC, $\Delta\lambda_k$,

$$\Delta\lambda_k = \lambda_{+,k} - \lambda_{-,k} = \frac{p_k g_n}{\omega_c(1 - g_n^2/4)}. \quad (4)$$

For an illustration, the transmission spectrum of a hetero-structure with $M = 4$, $N = 24$, $p_1 = 300$ nm, $n_1 = 1.45$, $n_2 = 2.00$ and $\theta = 0$ is calculated using the transfer matrix method [12] with a wavelength resolution of 0.001 nm and the result is shown in Fig. 5b (blue solid lines). There are three peaks in the transmission spectrum with the spacing between the two adjacent peaks increasing as k increases (as (4) suggests). The maximum values of the peaks are neither uniform nor equal to 1, as the overall transmission of the hetero-structure is a complex function of transmissions of all individual PCs.

Since the transmission spectrum in Fig. 5b consists of a broad range of wavelengths, it is important to include the refractive-index dispersions of the materials in the calculation. Let us assume the materials with the refractive indices $n_1 = 1.45$ and $n_2 = 2.0$ to be silica [13, 14] and amorphous silicon nitride ($a\text{-Si}_{1-x}\text{N}_x$) with $x = 0.455$ [14], respectively. The refractive-index dispersions of these materials can be obtained using Sellmeier equations [13, 14] and they are shown in Fig. 5c. In the wavelength range 1000–2400 nm (the range is indicated using black lines in Fig. 5c), the refractive index of amorphous silicon nitride changes by about 0.03 (from 2.00 (1000 nm) to 1.97 (2400 nm)). A similar change for silica is about 0.02. The red curve in Fig. 5b shows the transmission spectrum of the hetero-structure similar to that of the blue curve in Fig. 5b, however with the dispersions in Fig. 5c included. As we can see from Fig. 5b, the wavelengths and transmission values of the resonant peaks change slightly due to the material dispersion.

Finally, we would like to highlight the sensitivity of the band-edge resonance to the fluctuations in the layer thickness. For an analysis, let us assume a structure with the parameters as in Fig. 2 with $r = r_c$. The thickness of each dielectric layer in the 1D PC is taken as $L + r\Delta L$, where L is the thickness as in Fig. 2, r is a random number between -1 and 1 (different for different layers) and ΔL is the fluctuation parameter. Figure 6 shows the transmission plots, calculated using the transfer matrix method [12], with $\Delta L = 0.5$ nm, 1 nm and 2 nm. As we can see from the figure, when ΔL is increased, the transmission of the resonant peak drops and the line shape becomes more asymmetrical. Therefore, a good control of the layer thicknesses is necessary to ensure a resonant peak with high transmission and a symmetrical line shape.

The typical method to construct a narrow line width filter using 1D PCs is to use a defect layer between two identical 1D PCs [1, 2, 6]. The defect layer acts as a cavity and slows down the light. The photon lifetime of the cavity is about 1/FWHM of the filter. In our proposed structure, we achieved narrow line width filtering without any defect layers. Two 1D PCs with different periods are stacked together and the effect of band-edge resonance is used to construct the single channel narrow line width filter. It has to be noted

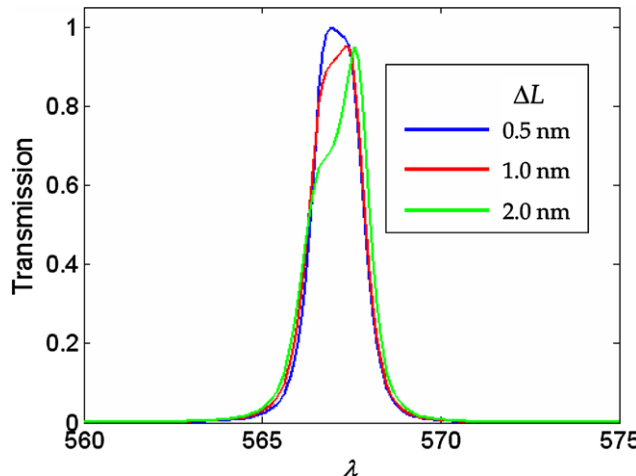


Fig. 6 Transmission spectra for hetero-structures with parameters as in Fig. 2 but with $r = r_c$ and fluctuating dielectric layer thicknesses

that, at the band-edge frequency, light travels with a very low group velocity [1, 2] and, therefore, has a finite lifetime. This low group velocity slows down the light and, hence, recreates the cavity effect which is found in the filters based on the defect layers in the 1D PCs. To construct a multichannel narrow line width filter based on the defect layer approach, a structure with multiple defect layers with each layer inserted between identical 1D PCs must be used [15, 16]. Following the approach in this paper, the construction of a multichannel narrow line width filter requires no defect layers, but multiple 1D PCs with different periods. The periods of the PCs must be designed such that all the adjacent band edges are in resonance. An important difference between the multichannel filters based on the defect layer approach and the band edge resonance approach is that, in the former, the spacing between the wavelength channels is lesser than the band-gap width of the 1D PC. In the filters based on the band edge resonance approach, the spacing between adjacent wavelength channels is equal to the band gap of one of the 1D PCs (see (4)). On the other hand, a common property that both filters (i.e. defect layer type and band edge resonance type) share is the dependence of the line width on the number of unit cells in each of the 1D PCs (i.e. N). For both filters, the line width decreases as N increases.

In conclusion, we have presented the design of narrow line width transmission filters using band edge resonance effects in a hetero-structure of 1D PCs. Band-edge resonance occurs when the upper and lower band edges of the adjacent PCs overlap. If the hetero-structure consists of M PCs with the periods being distributed in a geometrical progression of a common ratio, r_c , then the band-edge resonance causes $M - 1$ sharp resonant peaks to be formed in the transmission spectrum. These resonant peaks can be used to design narrow line width filters. The line width of the resonant peaks can be controlled by changing the refractive-index modulation and the number of unit cells in each PC. The paper also described the dependence of the resonance condition, r_c , on the incident angle and the polarization state of light.

References

1. A. Yariv, P. Yeh, *Optical Waves in Crystals* (Wiley, New York, 2003), Chap. 6
2. J.D. Joannopoulos, R.D. Meade, J.N. Winn, *Photonic Crystals: Molding the Flow of Light* (Princeton University Press, Princeton, 2008), Chap. 4
3. Y. Fink, J.N. Winn, S. Fan, C. Chen, J. Michel, J.D. Joannopoulos, E.L. Thomas, *Science* **282**, 1679 (1998)
4. J.N. Winn, Y. Fink, S. Fan, J.D. Joannopoulos, *Opt. Lett.* **23**, 1573 (1998)
5. E. Yablonovitch, *Opt. Lett.* **23**, 1648 (1998)
6. R. Ozaki, H. Moritake, K. Yoshino, M. Ozaki, *J. Appl. Phys.* **101**, 033503 (2007)
7. K.-Y. Xu, X. Zheng, W.-L. She, *Appl. Phys. Lett.* **85**, 6089 (2004)
8. Z.-Y. Wang, X.-M. Chen, X.-Q. He, S.-L. Fan, W.-Z. Yan, *Prog. Electromagn. Res.* **80**, 421 (2008)
9. D. Goldring, U. Levy, D. Mendlovic, *Opt. Express* **15**, 3156 (2007)
10. F. Villa, J.A. Gaspar-Armenta, *Opt. Express* **12**, 2338 (2004)
11. G. Alagappan, X.W. Sun, P. Shum, M.B. Yu, M.T. Doan, *J. Opt. Soc. Am. B* **23**, 159 (2006)
12. M. Born, E. Wolf, *Principles of Optics: Electromagnetic Theory of Propagation, Interference and Diffraction of Light* (Pergamon, London, 1999)
13. R.W. Waynant, *Electro-Optics Handbook* (McGraw-Hill, New York, 2000), Sect. 33.5
14. W.C. Tan, S. Kobayashi, T. Aoki, R.E. Johanson, S.O. Kasap, *J. Mater. Sci., Mater. Electron.* **20**, S15 (2009)
15. Q. Chen, D.W.E. Allsopp, *Opt. Commun.* **281**, 5771 (2008)
16. W. Li, L.-X. Chen, D. Tang, W. Ding, S. Liu, *Opt. Eng.* **46**, 064602 (2007)